

A Millimeter-Wave Current-Mode Inverse-Outphasing Transmitter Front-End

Sensen Li, *Student Member, IEEE*, and Hua Wang, *Senior Member, IEEE*
School of Electrical and Computer Engineering, Georgia Institute of Technology, USA

Abstract— The report presents a 28GHz current-mode inverse outphasing TX. Unlike the conventional voltage-mode outphasing using series power combiner, it employs current-mode PAs with parallel power combining, which facilitates its application at mm-Wave. The TX achieves 40%/31% PA efficiency at Psat (22.7dBm)/6dB PBO, showing 1.5× efficiency enhancement compared to an idealistic Class-B. Upto 15Gbit/s 64QAM is demonstrated in the modulation test, with 15.6dBm average Pout and 22.5% average PA efficiency.

Index Terms— Chireix compensation, CMOS, communication, efficiency enhancement, fifth-generation (5G), millimeter wave (mm-wave), outphasing, peak-to-average power ratio (PAPR), power amplifier (PA), transmitter (TX).

I. INTRODUCTION

AS mm-wave offers broader spectra and proportionate capacity increase, it will be extensively employed in 5G-and-beyond communication systems to address the exponentially growing data-rate demand. Viable mm-wave TX/PA solutions should handle multi-Gbit/s complex modulations with large PAPR, pushing the already stringent linearity-efficiency requirement on deployed TXs/PAs. This demand has stimulated extensive research on new TX/PA architectures to further advance the performance envelope at mm-wave.

Outphasing is a popular TX/PA topology to achieve large power-back-off (PBO) efficiency enhancement together with high peak efficiency. A typical outphasing architecture consists of two TX/PA branches that operate with their saturated voltage swings but dynamically varying phase difference to realize active load modulation at PBO [1]. However, two major challenges greatly limit the implementation and performance of conventional voltage-mode outphasing at mm-wave [2]. First, there is a lack of mm-wave series power combiners for low-loss voltage-mode outphasing load modulation. Recently, the on-antenna outphasing and triaxial-balun-based outphasing have been demonstrated at 28GHz, as two examples of mm-wave non-isolating outphasing series power combiners. Secondly, the conventional outphasing also requires two voltage-mode PAs with low output impedance. At mm-wave, they are approximated by overdriven Class-B common-source (CS) PAs, since standard voltage-mode PAs (e.g., Class-D PAs) are inefficient at mm-wave. This results in limited achievable Pout, linearity, and PAE at PBO. Moreover, overdriven CS PAs largely sacrifice the device power gain, which limits the use of conventional outphasing for high mm-wave applications, where device gain is highly precious and impacts efficiency directly.

On the other hand, many mm-wave TXs/PAs employ linear analog PAs (e.g. cascode-/stacked-PAs) due to their excellent gain/P_{out}/PAE trade-off, which however behave close to current sources with considerable output impedance.

II. MM-WAVE CURRENT-MODE INVERSE-OUTPHASING ARCHITECTURE AND ITS MEASUREMENT PERFORMANCE

To address these challenges, we propose a current-mode inverse outphasing architecture that supports compatibility with current-mode PAs, highly efficient active load modulation, and viable extension to high mm-wave. Figure 1a depicts the topologies of the conventional voltage-mode outphasing and the proposed current-mode inverse outphasing. In the conventional structure, two voltage sources drive a series power combiner. Shown in Fig. 1a, its equivalent parallel load resistance is modulated by the outphasing angle ϕ as $1/\cos 2\phi$. Meanwhile, ϕ -dependent complex-conjugate parallel reactances are formed in both outphasing paths, necessitating parallel reactance compensation at a pre-defined outphasing angle ϕ_c , i.e., the classic Chireix compensation. Specifically, in PBO, the phase leading path ($Ve^{j\phi}$) sees an inductive load, while the phase lagging path ($Ve^{-j\phi}$) observes a capacitive load, with the compensation angle ϕ_c determining the outphasing PBO level for efficiency peaking. In contrast, the proposed inverse outphasing is a circuit duality of the conventional outphasing architecture. Besides its use of current-sources driving, its outphasing power combiner is a parallel combiner that can be readily implemented as current combining at mm-wave. Moreover, instead of the equivalent admittance (Y), the equivalent impedance (Z) seen by each path should be evaluated, showing the series load resistance (R_s) is actively modulated by $\cos 2\phi$. Note that since the PA loads are modulated in an opposite fashion ($1/\cos^2\phi$ vs. $\cos^2\phi$), the outphasing angle ϕ of the proposed architecture should decrease for an increased load resistance at a larger PBO level, resulting in an inverse outphasing operation. In addition, the peak P_{out} requires the proposed architecture to operate at an outphased condition ($\pm\phi_0$), and thus the equivalent load is lowered by a factor of $\cos^2\phi_0$, which is particularly helpful for high-power mm-wave PA designs. Finally, since the inverse outphasing operations introduce ϕ -dependent series-load reactances, series Chireix compensations are necessary to cancel these reactances and achieve PBO efficiency enhancement.

The normalized P_{out} and effective PA load resistance versus outphasing angles are plotted in Fig. 1b. In the conventional voltage-mode outphasing, the PA output voltage swing is

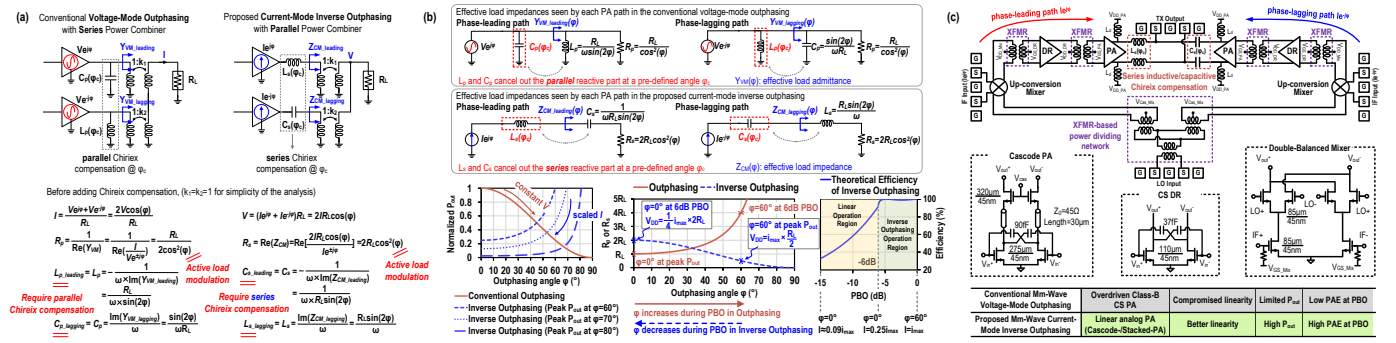


Fig. 1. (a) Conventional voltage-mode outphasing and proposed current-mode inverse outphasing. (b) Effective load impedances seen by each PA path in outphasing and inverse outphasing, and their operation comparison. (c) Top-level circuit schematic of the mm-wave current-mode inverse outphasing TX.

constant with increasing outphasing angle for PBO. In contrast, the proposed inverse outphasing decreases the outphasing angle together with properly scaled current amplitude to meet the load-line condition during PBO. Considering that practical outphasing angles are often restricted to $\phi \approx 60^\circ$ for improved efficiency, the load resistance R_p increases from R_L to $4R_L$ in the voltage-mode outphasing operation. In comparison, if we choose $\phi = 60^\circ$ for peak P_{out} in inverse outphasing, the PAs should achieve its maximum output voltage swing for optimal power/efficiency ($V_{DD} = i_{max} \times R_L / 2$). At 6dB PBO where ϕ decreases to 0° , the driving current amplitude reduces by 4x, again realizing full PA output voltage swing ($V_{DD} = i_{max} / 4 \times 2R_L$) for the 2nd efficiency peak. Beyond this PBO, the two PA paths operate as two in-phase analog PAs and achieve a large dynamic range as any analog PAs.

The top-level circuit schematic is shown in Fig. 1c. The phase-leading ($Ie^{j\phi}$) and phase-lagging ($Ie^{-j\phi}$) paths are parallel combined at the output, with the series inductive and capacitive Chirex compensation at the corresponding path. Each path consists of a cascode PA, a CS driver (DR), and an up-conversion mixer. The cascode PA is used for its higher P_{out} and power gain, and its high output impedance is inherently accommodated by the inverse outphasing architecture. The double-balanced mixers up-convert the 5GHz IF signals to the 28GHz carrier. Transformers are used as inter-stage matching, with center taps for biasing and common-mode terminations.

The measured CW performance is summarized in Fig. 2a. At 29GHz, the TX achieves 22.7dBm peak P_{out} , with 42.6/35.5/33.6% for the PA-only, PA+DR, and total TX peak drain efficiency (η_D), respectively. At 6dB PBO, a 31% PA-only η_D is achieved, demonstrating 1.5x efficiency enhancement over an ideal Class-B PA. To characterize the AM-AM/AM-PM nonlinearity behaviors of the TX, the output of the TX is first attenuated and then down-converted by an external mixer, with the LO driven by the same signal source in the up-conversion. The down-converted signal is sent to a real-time sampling oscilloscope and is compared with a coherent reference signal. The reference signal and the trigger signal for the sampling oscilloscope are from the other two channels of the 4-channel AWG. A memoryless 2-D (P_{in}, ϕ) lookup table (LUT) is thus generated, providing the desired input outphased signals and performing a one-step DPD to correct the AM-AM/AM-PM errors. Over the frequency, the TX delivers more than 20dBm P_{out} from 26 to 32GHz, maintaining above 32%

PA-only, 25% PA+DR, and 23% total TX drain efficiency η_D . Figure 2b summarizes the modulation testing results with a single-carrier 64-QAM signal. When transmitting a 13.5Gb/s 64-QAM signal, the inverse outphasing TX achieves -23.5dB EVM_{RMS} and 29.4dB ACLR with an average P_{out}/η_D (PA) of 15.2dBm/22.2%, demonstrating the state-of-the-art modulation bandwidth and average P_{out} /efficiency among reported silicon-based outphasing PAs/TXs in the same frequency band.

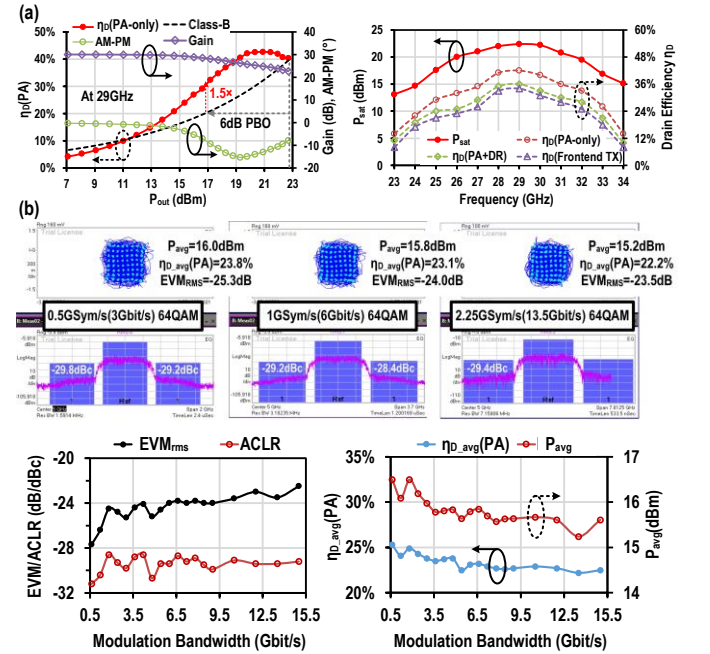


Fig. 2. Measurement results of the inverse outphasing TX.

III. CAREER PLAN AND FELLOWSHIP IMPACT

I am honored and grateful to receive the fellowship, which offered me the chance to attend IMS learning the cutting-edge microwave technologies, and further motivated me to pursue a career in microwave engineering. I plan to continue my research after graduation in either industry or academia.

REFERENCES

- [1] S. Li *et al.*, "A 28-GHz Flip-Chip Packaged Chirex Transmitter with On-Antenna Outphasing Active Load Modulation," *IEEE Journal of Solid-State Circuits*, vol. 54, no. 5, pp.1243-1253, May 2019.
- [2] S. Li *et al.*, "A 28GHz Current-Mode Inverse-Outphasing Transmitter Achieving 40%/31% PA Efficiency at $P_{sat}/6dB$ PBO and Supporting 15Gbit/s 64-QAM for 5G Communication," in *IEEE Int. Solid-State Circuits Conf. (ISSCC) Dig. Tech. Papers*, Feb. 2020, pp. 366-368.